



RESEARCH LETTER

10.1002/2014GL061249

Key Points:

- A localized LVZ in the lowermost mantle beneath Kamchatka is detected
- Such low-velocity anomaly is not observed in most regions
- It may represent a mantle plume undetected before in the lower mantle

Supporting Information:

- Readme
- Figure S1
- Figure S2
- Figure S3
- Figure S4
- Figure S5

Correspondence to:

Y. He,
ymhe@mail.igcas.ac.cn

Citation:

He, Y., L. Wen, and T. Zheng (2014), Seismic evidence for an 850 km thick low-velocity structure in the Earth's lowermost mantle beneath Kamchatka, *Geophys. Res. Lett.*, 41, doi:10.1002/2014GL061249.

Received 17 JUL 2014

Accepted 1 OCT 2014

Accepted article online 2 OCT 2014

Seismic evidence for an 850 km thick low-velocity structure in the Earth's lowermost mantle beneath Kamchatka

Yumei He¹, Lianxing Wen^{2,3}, and Tianyu Zheng¹

¹Key Laboratory of Earth and Planetary Physics, Institute of Geology and Geophysics, Chinese Academy of Sciences, Beijing, China, ²Department of Geosciences, State University of New York at Stony Brook, Stony Brook, New York, USA, ³Laboratory of Seismology and Physics of Earth's Interior, School of Earth and Space Sciences, University of Science and Technology of China, Hefei, China

Abstract We detect an 850 km thick low-velocity structure in the Earth's lowermost mantle beneath Kamchatka surrounded by and overlying a 210 km thick high-velocity D'' structure. The velocity structure is constrained by modeling the observed anomalously broadened waveforms for seismic shear waves sampling the lowermost mantle recorded at large distances from 90° to 100°. Waveform modeling analyses reveal that the low-velocity anomaly has a stem with a diameter of about 550 km in the lowermost 210 km of the mantle and a cap with a diameter of about 1600 km. The low-velocity structure of the cap decreases from 0% at the top to -1.5% at about 400 km above the core-mantle boundary (CMB) and to -1.2% at 210 km above the CMB. We suggest that the geometrical and velocity features of the low-velocity anomaly indicate that it may represent a localized mantle plume undetected before in the lower mantle.

1. Introduction

Seismic studies have consistently shown the existence of two large-scale low shear velocity provinces near the core-mantle boundary (CMB) beneath Africa and Pacific Ocean (the African Anomaly and Pacific Anomaly) [Montelli et al., 2006; Kustowski et al., 2008; Simmons et al., 2010; Ritsema et al., 2010]. Both Anomalies occupy broad areas at the CMB, extend to the mid-lower mantle with sharp edges, have shear velocity perturbations varying from -3% at the top to -5% (the Pacific Anomaly) and -12% (the African Anomaly) at the CMB, and are likely chemically distinct [Wen et al., 2001; Wen, 2001; Ni et al., 2002; To et al., 2005; Wang and Wen, 2007; He and Wen, 2009; Sun et al., 2009]. The existence of two chemical anomalies in the lowermost mantle has inspired many studies on thermochemical convection in the mantle [McNamara and Zhong, 2005; Tackley, 2012], early differentiation process of the Earth [Wen et al., 2001; Labrosse et al., 2007], relationship of thermochemical plumes with surface hotspots [Wen, 2006; Torsvik et al., 2010; Tan et al., 2011; Steinberger and Torsvik, 2012], and the origin of geochemical DUPAL anomalies at the Earth's surface [Wen, 2006]. Recently, waveform analysis also suggested the existence of a small-scale low-velocity structure near the CMB beneath Perm (the Perm Anomaly) and proposed that it has a similar origin as the African and Pacific Anomalies [Lekic et al., 2012]. Continued efforts to search for the existence of small-scale low-velocity anomalies would further improve our understanding of the origin of seismic anomalies and dynamic processes in the lowermost mantle.

Seismic waveforms in the distance range of 80°-110° are sensitive to the shear velocity structure in the lowermost mantle [e.g., Wen et al., 2001; Wen, 2002; He and Wen, 2012; Sun and Miller, 2013]. In this study, we present seismic observations of anomalously broadened SH and SV waveforms for the seismic data sampling the lower mantle beneath Kamchatka. Forward two-dimensional (2-D) waveform modeling of the seismic data suggests existence of a localized 850 km thick low shear velocity anomaly in the lowermost mantle beneath Kamchatka, surrounded by and overlying a high-velocity D'' region. We present seismic data in section 2, seismic modeling results in section 3, and possible origins of the low-velocity structure in section 4.

2. Seismic Data

We collected broadband tangential and radial displacements of S and S_{diff} phases recorded at a distance range between 80° and 110° for all the events sampling outside the Pacific and African Anomalies, occurring

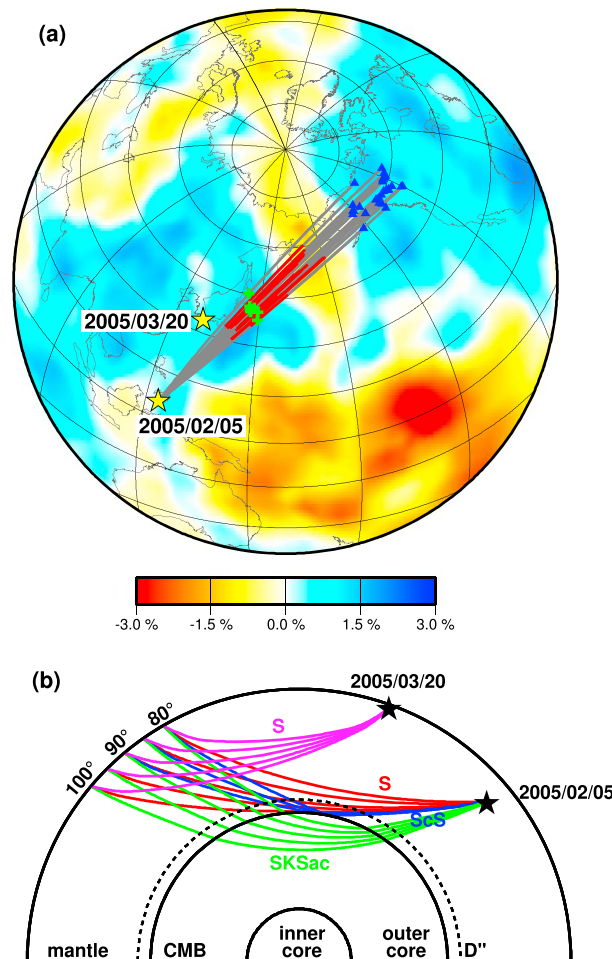


Figure 1. (a) The selected event 2005/02/05 used in this study (yellow star), S, S_{diff} raypaths propagating in the lowermost 200 km of the mantle (red bold lines), seismic stations (blue triangles), ScS bouncing points at the CMB (green crosses), and great circle paths (gray lines), along with a reference earthquake 2005/03/20 (yellow star). Tomographic shear velocity perturbations at the CMB are also plotted as background [Simmons *et al.*, 2010]. (b) Raypaths of direct S at epicentral distances from 50° to 70° (purple lines) for event 2005/03/20 and raypaths of direct S, S_{diff} at epicentral distances from 80° to 100° (red lines), ScS at epicentral distances from 80° to 90° (blue lines), and SKS at epicentral distances from 80° to 100° (green lines) for event 2005/02/05. These raypaths are calculated on the basis of PREM.

on preliminary reference Earth model (PREM) [Dziewonski and Anderson, 1981] (Figure 2a). ScS phases can be observed from 82° to 86°. There exists three strong seismic phases from 90° to 100° (Figure 2a), exhibiting the same polarity and comparable amplitudes. The first phase (labeled as S1) emerges at 90° and exhibits faster than the normal SH arrival times from 0 s at 90° to 2 s at 100°; the second phase (labeled as S2) has travel time delays from 1.5 s at 90° to 3 s at 100°, and the third phase (labeled as S3) has travel time delays from 4 s at 90° to 8 s at 100°. The existence of these phases significantly broadens the SH waveforms.

The waveform complexities of event 2005/02/05 are most likely caused by the seismic heterogeneities in the lowermost mantle, as they cannot be explained by other factors, such as mislocation of the earthquake, complexities of source time function, and the seismic heterogeneities in the source side mantle. Mislocation of the earthquake and a complex source would result in a uniform travel time delay and similar waveform complexities across the stations, which are different from the observations. Near-station effects and the

from 1994 to 2013 with a magnitude greater than 5.8 and focal depth greater than 50 km. All seismic data are collected from the Incorporated Research Institutions for Seismology (IRIS). After visual inspection of all available data, we identify anomalously broadened S, S_{diff} waveforms for an event (2005/02/05) with a simple source time function and high signal-to-noise ratios. The event occurred in Mindanao, Philippines, and is recorded in Alaska and Canada, and mostly by the Canadian Northwest Experiment deployed from 25 May 2003 to 23 September 2005. All data are deconvolved with their instrumental response and band-pass filtered from 0.008 to 0.2 Hz.

3. Seismic Velocity Structure in the Lower Mantle Beneath Kamchatka

The seismic waves of event 2005/02/05 sample the lowermost mantle beneath Kamchatka peninsula within an azimuthal range from 23° to 38° (Figure 1). We first redetermine location and origin time of the earthquake (see Table 1); we then correct for the travel time residuals that are caused by the seismic heterogeneities 500 km above the CMB based on tomographic model GyPSuM [Simmons *et al.*, 2010] and seismic data of an event (2005/03/20) closer to the stations as reference (Table 1 and Figures 1 and S1 in the supporting information). The corrections are made following a procedure similar to that in He and Wen [2009], with details presented in the supporting information.

SH phases of event 2005/02/05 exhibit travel time delays from 0 s at 82° to 1.5 s at 86° with respect to the predictions based

Table 1. Events List^a

Event	Origin Time	Latitude (°N)	Longitude (°E)	Depth (km)	Time Correction (s)
2005/02/05	2005.036.12.23.19	5.47(5.22)	123.67(123.67)	531(532)	-2.0
2005/03/20	2005.079.01.53.42	33.81(33.71)	130.13(130.03)	10(8)	1.0

^aValues in parentheses are relocated latitude, longitude, and depth.

upper mantle structure beneath Alaska and Canada appear to contribute little to the complexities as well, because the records at the same stations for one earthquake 2005/03/20 occurring in Kyushu, Japan, show simple waveforms (Figures 1 and S2 in the supporting information). Moreover, the SKS phases of the same event (2005/02/05) show simple and similar waveforms across the stations, ruling out the possibility that the waveform complexities are due to the effects of the receiver side crust and upper mantle heterogeneities (Figure S3 in the supporting information).

We first adopt one-dimensional (1-D) waveform modeling analysis to illustrate the relationship of velocity structures in the lowermost mantle to the diagnostic features observed in the seismic data, since 1-D waveform propagation is easier to be understood. We apply the method of Generalized Ray Theory to calculate synthetic seismograms with a 6.5 s wide trapezoid source time function [Helmberger, 1983]. Forward 1-D waveform modeling suggests that the seismic data can be explained by a localized low-velocity anomaly situated above a high-velocity D'' layer in the lowermost mantle (Figure 2c). A model that has a velocity jump of 2.0% at 220 km above the CMB can explain the strong S1 phase (Scd phase in the synthetics, Figure 2b) in the distance range larger than 90°. S3 phase can be explained by S wave refractions in the low-velocity layer with a thickness of 540 km and a velocity reduction of -1.2% located above the bottom high-velocity layer (Sab phase in the synthetics, Figure 2b). S2 phase can be explained by S wave reflection off the top of D'' layer (Sbc phase in the synthetics, Figure 2b). Both the low-velocity zone and D'' high-velocity layer are needed to explain the observed waveform complexities. A model with a 220 km thick high-velocity layer alone would produce anomalously broadened waveforms in the distance range between 90° and 100°.

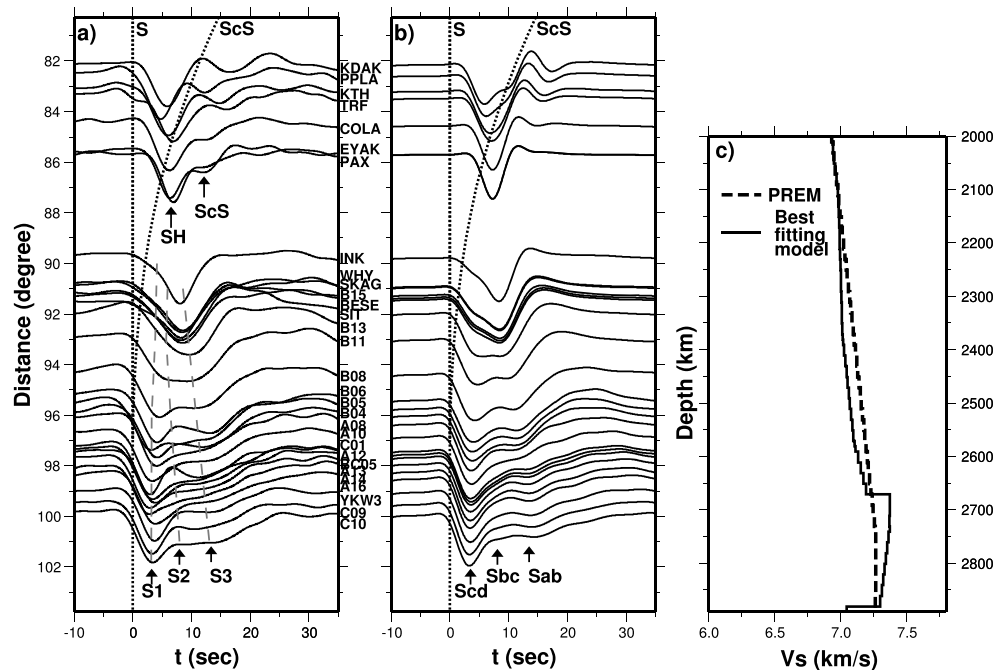


Figure 2. (a) Observed tangential displacements for event 2005/02/05 sampling the lowermost mantle beneath Kamchatka. Some observed phases are labeled (SH, ScS, and S1-S3 for discussion purposes) and indicated by arrows. Gray dashed lines follow the troughs of S1-S3 phases. (b) Synthetics calculated based on the 1-D model shown in Figure 2c. The calculated Sab, Sbc, and Scd phases are indicated by arrows. (c) The best fitting 1-D shear velocity model along with PREM.

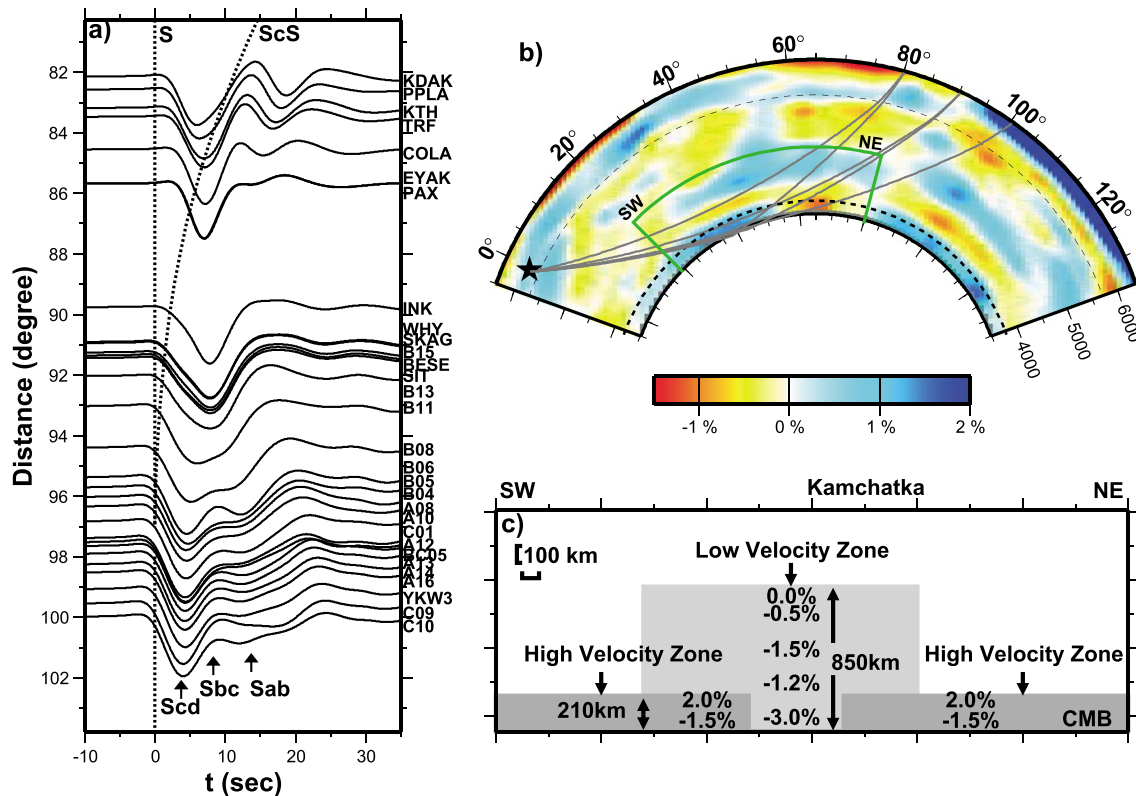


Figure 3. (a) Synthetics for event 2005/02/05 calculated based on the 2-D model shown in Figure 3c. The calculated Sab, Sbc, and Scd phases are indicated by arrows. (b) Two-dimensional cross section along the great circle path in Figure 1a of global tomographic model GYPsuMS [Simmons *et al.*, 2010], earthquake (black star), raypaths of S, S_{diff} phases at epicentral distances from 80° to 100° (gray lines), and S_{cS} at epicentral distances from 80° to 90° (gray lines). The 2-D model domain of Figure 3c is shown in green lines. (c) The inferred 2-D model.

However, it would also produce much earlier Sab, Sbc, and Scd arrival times and narrower Sab phases, different from the observed waveforms (Figure S4 in the supporting information). A low-velocity layer above the D'' high-velocity layer is needed to fit the phase arrival times and produce broadened Sab phase. The thickness of the low-velocity layer is constrained to be at least greater than 450 km and the shear velocity reduction between -1.5% and -1%. A smaller thickness would not generate Sab phases with proper width and amplitudes as well as travel time delays to fit the data; a velocity reduction greater than -1.5% would produce too strong Sab phase and too large travel time delays of Sab phases to fit the observations, while a velocity reduction lower than -1.0% would produce too small travel time delays of Sab phases to fit the data. Furthermore, a velocity reduction at the top of the low-velocity layer should be less than -0.5%, as a greater value would generate a distinguishable postcursor (labeled as Sp, Figure S5 in the supporting information) after Sab phase, which is not observed in the data.

The best fitting 1-D model has a 540 km thick low shear velocity zone situated above a 220 km thick high-velocity region in the CMB. The low-velocity structure has velocity reductions varying from 0% at the top to -1.2% at 510 km above the CMB followed by an average shear velocity reduction of -1.2% to 310 km above the CMB then a decrease of velocity reduction to -0.5% at 220 km above the CMB (Figure 2c). The high-velocity structure has a discontinuity with a velocity jump of 2.0% at 220 km above the CMB followed by a negative gradient from 2.0% to 0.5% at 10 km above the CMB and a velocity reduction of -3% in the bottom 10 km of the mantle (Figure 2c).

We construct a 2-D model of the cross section by taking reference of the main velocity features of the inferred best fitting 1-D model and lateral variation of seismic structure revealed in tomographic model GYPsuMS [Simmons *et al.*, 2010]. Tomographic model GYPsuMS suggests existence of a thick low-velocity anomaly in the lowermost mantle beneath Kamchatka surrounded by about 300 km thick D'' high-velocity structures (Figure 3b). We therefore test a series of 2-D models with a thick localized low-velocity anomaly beneath

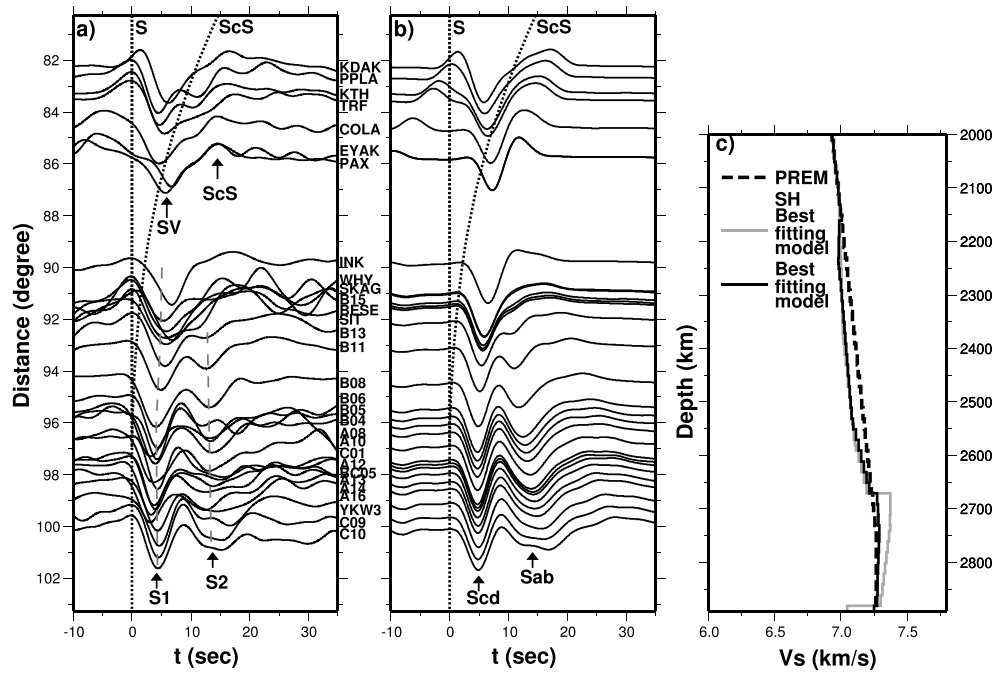


Figure 4. (a) Observed radial displacements for event 2005/02/05 sampling the lowermost mantle beneath Kamchatka. Some observed phases are labeled (SH, ScS, and S1 and S2 for discussion purpose) and indicated by arrows. Gray dashed lines follow the troughs of S1 and S2 phases. (b) Synthetics calculated based on the 1-D model shown in Figure 3c. The calculated Sab and Scd phases are indicated by arrows. (c) The best fitting 1-D SV shear velocity model, along with PREM and the best fitting 1-D SH shear velocity model in Figure 2c.

Kamchatka surrounded by a high-velocity D'' layer. Various geometries (mushroom shaped, cone shaped, rectangle shaped, and inverted trapezoid shaped), heights, and locations of the low-velocity anomaly are tested. The velocity structures of the low-velocity anomaly and the D'' layer are perturbed from those in the inferred best fitting 1-D model (Figure 2c). The SH hybrid method is applied to calculate synthetic seismograms [Wen, 2002], with source mechanism obtained from the Harvard centroid moment tensor catalog [Dziewonski et al., 1981].

In the best fitting 2-D model, the low-velocity structure is 850 km high and has a stem with a diameter of about 550 km in the lowermost 210 km of the mantle and a wide cap with a diameter of about 1600 km extending to 850 km above the CMB. The thickness of the low-velocity structure is constrained by the broadened Sab phase. Though there exists trade-off between the width of the cap and detailed velocity structure and a cap with a diameter of 1400 km or 1800 km with slightly different velocity structure that can produce synthetics fitting the observation equally well, a wide cap with a low-velocity zone situated above the bottom high-velocity structure is needed to produce Sbc and Sab phases with comparable amplitudes as those of Scd phases to fit the observations. Due to the finite width of the low-velocity cap, the 2-D model also produces earlier Scd phase at station KDAK and better fits the observations (Figures 2b and 3a). Above the D'' layer, the low-velocity anomaly has a similar velocity structure as the best fitting 1-D model, with velocity reductions varying from 0% at the top to -1.5% at about 400 km above the CMB and to -1.2% at 210 km above the CMB. The velocity structure of the stem of the low-velocity anomaly at the bottom 210 km of the mantle varies from -1.2% at the top to -3% at the CMB (Figure 3c). The high-velocity structure has a discontinuity at 210 km above the CMB with a velocity jump of 2.0%, followed by a negative gradient from 2.0% to 1.0% at 90 km above the CMB and a decrease of velocity reduction to -1.5% at the CMB.

Radial displacement seismograms of event 2005/02/05 also show anomalous SV waveforms from 90° to 100° (Figure 4a). The first phase (labeled S1) exhibit little travel time delays from 90° to 100° with respect to the PREM predictions. There exists one strong phase (labeled S2) after S1 phase from 92° to 100°. This phase exhibits the same polarity and comparable amplitude as S1 phases, with travel time delays varying from 7.5 s at 92° to 9 s at 100°. By fixing the thickness of the high-velocity structure to be 220 km, forward waveform

modeling shows that the best fitting model consists of a similar low-velocity structure above the D'' discontinuity but with a different high-velocity structure at the base (Figures 2c and 4c). The high-velocity structure has a small-velocity jump of 0.5% at 220 km above the CMB followed by a negative gradient from 0.5% to 0.1% at 10 km above the CMB and a velocity reduction of -0.2% in the bottom 10 km of the mantle (Figures 4b and 4c).

4. Mantle Plume as a Possible Explanation

The low-velocity anomaly with a cap of a large-lateral dimension and a narrow stem is consistent with plume morphology, and the velocity gradient in the top portion of the anomaly (from 0% at the top to -1.5% at about 400 km above the CMB) is consistent with a thermal boundary layer developed at the top of a plume. We thus suggest that the low-velocity anomaly may represent a mantle plume undetected before in the lower mantle. The inferred SH D'' structure is similar to those reported in other regions [e.g., *Young and Lay, 1987; Young and Lay, 1990; Gaherty and Lay, 1992; Weber, 1993; Kendall and Shearer, 1994; Ding and Helmberger, 1997; Wysession et al., 1998; Lay, 2007; He and Wen, 2011*]. The different velocity jumps of 2.0% (SH) and 0.5% (SV) at the D'' discontinuity may be caused by anisotropy of the postperovskite phase [*Nowacki et al., 2011*]. If the presence of a D'' layer is related to an ancient slab at the CMB, the seismic structure may also indicate complex interaction between the subducted slab and development of mantle plume in the lowermost mantle.

Interestingly, a similar low-velocity structure above the D'' discontinuity was also reported in many previous 1-D D'' models, such as SGLE for northern Asia and SYLO for Alaska [*Young and Lay, 1990; Gaherty and Lay, 1992*]. However, as we show that such a low-velocity structure can be best resolved by the seismic waveforms at large distances from 90° to 100° , the seismic data at these distances were not used in constraining those previous models. So the low-velocity structure in the previous 1-D models was probably introduced to compensate the arrival time of some phases, and it is likely not a well-resolved feature. In fact, some studies even speculated that it was an artifact that resulted from embedding the discontinuity in a smooth reference model [*Wysession et al., 1998; Lay, 2007*]. Nevertheless, as we show in this study, localized low-velocity structures do exist at those depths. Thus, some of these previously reported structures may be real and may be validated and refined with an extensive global search for the anomalous waveform features at large distances from 90° to 100° . With their refined morphologic features, it may also assist identification of some undetected localized mantle plumes among these anomalies.

5. Conclusion

We observe anomalously broadened SH and SV waveforms for the seismic data sampling the lowermost mantle beneath Kamchatka. Forward 2-D waveform modeling analyses reveal existence of an 850 km thick low-velocity anomaly surrounded by and overlying a 210 km thick high-velocity D'' structure. The anomaly has a stem with a diameter of about 550 km in the lowermost 210 km of the mantle and a cap with a diameter of about 1600 km. The low-velocity structure of the cap decreases from 0% at the top to -1.5% at about 400 km above the CMB and to -1.2% at 210 km above the CMB. The velocity structure of the stem at the bottom 210 km of the mantle varies from -1.2% at the top to -3% at the CMB. We suggest that the geometrical and velocity structures of the low-velocity anomaly indicate that it may represent a localized mantle plume undetected before in the lower mantle.

Acknowledgments

We gratefully acknowledge the participants of the IRIS for its efforts in collecting the data. We thank Michael Wysession and two anonymous reviewers for comments and suggestions that improved the paper significantly. Figures were made with the General Mapping Tools [*Wessel and Smith, 1995*]. This work was supported by the National Science Foundation of China (grant 41125015) and Chinese Academy of Sciences and NSF grants 0911319 and 1214215.

Michael Wysession thanks two anonymous reviewers for their assistance in evaluating this paper.

References

- Ding, X., and D. V. Helmberger (1997), Modelling D'' structure beneath Central America with broadband seismic data, *Phys. Earth Planet. Inter.*, *101*, 245–270.
- Dziewonski, A. M., and D. L. Anderson (1981), Preliminary Reference Earth model, *Phys. Earth Planet. Inter.*, *25*, 297–356, doi:10.1016/0031-9201(81)90046-7.
- Dziewonski, A. M., T.-A. Chou, and J. H. Woodhouse (1981), Determination of earthquake source parameters from waveform data for studies of global and regional seismicity, *J. Geophys. Res.*, *86*, 2825–2852, doi:10.1029/JB086iB04p02825.
- Gaherty, J. B., and T. Lay (1992), Investigation of laterally heterogeneous shear velocity structure in D'' beneath Eurasia, *J. Geophys. Res.*, *97*(B1), 417–435, doi:10.1029/91JB02347.
- He, Y., and L. Wen (2009), Structural features and shear-velocity structure of the "Pacific Anomaly", *J. Geophys. Res.*, *114*, B02309, doi:10.1029/2008JB005814.
- He, Y., and L. Wen (2011), Seismic velocity structures and detailed features of the D'' discontinuity near the core-mantle boundary beneath eastern Eurasia, *Phys. Earth Planet. Inter.*, *189*, 176–184.

- He, Y., and L. Wen (2012), Geographic boundary of the "Pacific Anomaly" and its geometry and transitional structure in the north, *J. Geophys. Res.*, *117*, B09308, doi:10.1029/2012JB009436.
- Helmberger, D. V. (1983), Theory and application of synthetic seismograms, in *Earthquakes: Observation, Theory and Interpretation*, edited by H. Kanamori, pp. 173–222, Soc. Ital. di Fis., Bologna, Italy.
- Kendall, J.-M., and P. M. Shearer (1994), Lateral variations in D'' thickness from long-period shear wave data, *J. Geophys. Res.*, *99*, 11,575–11,590, doi:10.1029/94JB00236.
- Kustowski, B., G. Ekström, and A. M. Dziewoński (2008), Anisotropic shear-wave velocity structure of the Earth's mantle: A global model, *J. Geophys. Res.*, *113*, B06306, doi:10.1029/2007JB005169.
- Labrosse, S., J. W. Hernlund, and N. Coltice (2007), A crystallizing dense magma ocean at the base of the Earth's mantle, *Nature*, *450*, 866–869, doi:10.1038/nature06355.
- Lay, T. (2007), Deep Earth structure: Lower mantle and D'', in *Treatise on Geophysics*, vol. 1, *Seismology and Structure of the Earth*, edited by B. Romanowicz and A. Dziewoński, chap. 1.18, pp. 619–654, Elsevier, Amsterdam, Netherlands.
- Lekic, V., S. Cottar, A. Dziewoński, and B. Romanowicz (2012), Cluster analysis of global lower mantle tomography: A new class of structure and implications for chemical heterogeneity, *Earth Planet. Sci. Lett.*, *357–358*, 68–77.
- McNamara, A. K., and S. Zhong (2005), Thermochemical structures beneath Africa and the Pacific Ocean, *Nature*, *437*, 1136–1139, doi:10.1038/nature04066.
- Montelli, R., G. Nolet, A. Dahlen, and G. Masters (2006), A catalogue of deep mantle plumes: New results from finite-frequency tomography, *Geochem. Geophys. Geosyst.*, *7*, Q11007, doi:10.1029/2006GC001248.
- Ni, S., E. Tan, M. Gurnis, and D. Helmberger (2002), Sharp sides to the African superplume, *Science*, *296*, 1850–1852.
- Nowacki, A., J. Wookey, and J.-M. Kendall (2011), New advances in using seismic anisotropy, mineral physics and geodynamics to understand deformation in the lowermost mantle, *J. Geodyn.*, *52*, 205–228.
- Ritsema, J., A. Duess, H. J. van Heijst, and J. H. Woodhouse (2010), S40RTS: A degree-40 shear-velocity model for the mantle from new Rayleigh wave dispersion, teleseismic traveltime and normal-mode splitting function measurements, *Geophys. J. Int.*, doi:10.1111/j.1365-246X.2010.04884.x.
- Simmons, N. A., A. M. Forte, L. Boschi, and S. P. Grand (2010), GyPSuM: A joint tomographic model of mantle density and seismic wave speeds, *J. Geophys. Res.*, *115*, B12310, doi:10.1029/2010JB007631.
- Steinberger, B., and T. H. Torsvik (2012), A geodynamic model of plumes from the margins of Large Low Shear Velocity Provinces, *Geochem. Geophys. Geosyst.*, *13*, Q01W09, doi:10.1029/2011GC003808.
- Sun, D., and M. S. Miller (2013), Study of the western edge of the African Large Low Shear Velocity Province, *Geochem. Geophys. Geosyst.*, *14*, 3109–3125, doi:10.1002/ggge.20185.
- Sun, D., D. Helmberger, S. Ni, and D. Bower (2009), Direct measures of lateral velocity variation in the deep mantle, *J. Geophys. Res.*, *114*, B05303, doi:10.1029/2008JB005873.
- Tackley, P. J. (2012), Dynamics and evolution of the deep mantle resulting from thermal, chemical, phase and melting effects, *Earth Sci. Rev.*, *110*, 1–25.
- Tan, E., W. Leng, S. Zhong, and M. Gurnis (2011), On the location of plumes and lateral movement of thermochemical structures with high bulk modulus in the 3-D compressible mantle, *Geochem. Geophys. Geosyst.*, *12*, Q07005, doi:10.1029/2011GC003665.
- To, A., B. Romanowicz, Y. Capdeville, and N. Takeuchi (2005), 3D effects of sharp boundaries at the borders of the African and Pacific superplumes: Observations and modeling, *Earth Planet. Sci. Lett.*, *233*, 137–153, doi:10.1016/j.epsl.2005.01.037.
- Torsvik, T. H., K. Burke, B. Steinberger, S. J. Webb, and L. D. Ashwal (2010), Diamonds sampled by plumes from the core-mantle boundary, *Nature*, *466*, 352–355, doi:10.1038/nature09216.
- Wang, Y., and L. Wen (2007), Geometry and P and S velocity structure of the "African Anomaly", *J. Geophys. Res.*, *112*, B05313, doi:10.1029/2006JB004483.
- Weber, M. (1993), P- and S-wave reflections from anomalies in the lowermost mantle, *Geophys. J. Int.*, *115*, 183–210, doi:10.1111/j.1365-246X.1993.tb05598.x.
- Wen, L. (2001), Seismic evidence for a rapidly varying compositional anomaly at the base of the Earth's mantle beneath the Indian Ocean, *Earth Planet. Sci. Lett.*, *194*, 83–95.
- Wen, L. (2002), An SH hybrid method and shear velocity structures in the lowermost mantle beneath the central Pacific and south Atlantic oceans, *J. Geophys. Res.*, *107*(B3), doi:10.1029/2001JB000499.
- Wen, L. (2006), A compositional anomaly at the Earth's core-mantle boundary as an anchor to the relatively slowly moving surface hotspots and as source to the DUPAL anomaly, *Earth Planet. Sci. Lett.*, *246*, 138–148.
- Wen, L., P. Silver, D. James, and R. Kuehnel (2001), Seismic evidence for a thermo-chemical boundary at the base of the Earth's mantle, *Earth Planet. Sci. Lett.*, *189*, 141–153.
- Wessel, P., and W. H. F. Smith (1995), New version of the Generic Mapping Tools released, *Eos. Trans. AGU*, *76*(33), 329.
- Wysession, M. E., T. Lay, J. Revenaugh, Q. Williams, E. J. Garnero, R. Jeanloz, and L. H. Kellogg (1998), The D'' discontinuity and its implications, in *The Core-Mantle Boundary Region*, *Geodyn. Ser.*, vol. 28, edited by M. Gurnis et al., pp. 273–298, AGU, Washington, D. C.
- Young, C. J., and T. Lay (1987), Evidence for a shear velocity discontinuity in the lower mantle beneath India and the Indian Ocean, *Phys. Earth Planet. Inter.*, *49*, 37–53.
- Young, C. J., and T. Lay (1990), Multiple phase analysis of the shear velocity structure in the D'' region beneath Alaska, *J. Geophys. Res.*, *95*(B11), 17,385–17,402, doi:10.1029/JB095iB11p17385.